Unveiling design criteria of hollow fibers dielectric elastomer actuators
a computational and experimental study

Jafarzadeh, Sina; Gökova, Maxim; Kang, Zhaoqing; Yu, Liyun; Skov, Anne Ladegaard

Published in:
Proceedings of SPIE

Link to article, DOI:
10.1117/12.3010130

Publication date:
2024

Document Version
Publisher's PDF, also known as Version of record

Unveiling design criteria of hollow fibers dielectric elastomer actuators: a computational and experimental study

Sina Jafarzadeh[a], Maxim Gökova[a], Zhaoqing Kang[a], Liyun Yu[a], Anne Ladegaard Skov [a]*

[a] Danish Polymer Centre, Department of Chemical and Biochemical Engineering, Technical University of Denmark, Kongens Lyngby, Denmark

* Corresponding author: al@kt.dtu.dk; phone +45 23652156

ABSTRACT

Dielectric elastomer actuators (DEAs) have been proclaimed as a transformative technology with applications spanning from robotics to biomedical devices. They are especially appealing because of their key characteristics, including low weight and lifetime. However, there are still challenges in tuning these actuators for desirable mechanical performance. Here, we examine the effects of geometry and material characteristics like inner diameter and Young's modulus on the performance of hollow fiber dielectric elastomer actuators (HFDEAs). These parameters were chosen because they are amenable to experimental validation and play a straightforward, yet significant, role in DEA performance. The model's parameters are based on experimental data, giving our computational simulations a solid foundation. The study takes into consideration the electro-mechanical coupling using finite element method (FEM) simulations in COMSOL Multiphysics. While the electrodes' attraction to one another results in length expansion, the results suggest that the larger surface charge density on the internal electrode compared to the inner one in hollow fiber DEAs results in radial expansion as well. This model also provides an estimation on the actuator holding force which is challenging to evaluate experimentally. According to preliminary results, careful parameter selection can indeed increase the holding force, thereby enhancing the actuator's overall effectiveness. In conclusion, this study provides an understanding of design parameters of HFDEA offering a comprehensive framework for HFDEA design by integrating both experimental and computational approaches.

Keywords: Dielectric Elastomer Actuators (DEAs), Finite Element Method (FEM), Electro-Mechanical Modeling, Hollow Fiber Actuators, Hollow Fiber Dielectric Elastomer Actuators (HFDEAs).

1. INTRODUCTION

The field of soft robotics has garnered considerable attention from the research community due to its potential for innovative applications. Soft robots, constructed from compliant materials, exhibit remarkable mechanical resilience and adaptability to varying environments, alongside ensuring safety when interacting with humans. These characteristics hold promise for various applications, including natural environment exploration and rescue operations, industrial object manipulation, and human assistance in rehabilitation scenarios[1]–[3].

Among the various actuation technologies propelling the advancement of soft robotics, Dielectric Elastomer Actuators (DEAs) stand out due to their promising attributes [4]–[7]. DEAs, comprising an elastomer membrane encapsulated by two compliant electrodes, facilitate rapid actuation and high electro-mechanical conversion efficiencies, with the application of a high voltage inducing opposite charges on these electrodes. This action results in the membrane being compressed along its thickness while expanding along its planar dimensions, achieving speeds up to 600 Hz and theoretical efficiencies up to 90%, alongside substantial actuation strains exceeding 1000% [8]–[10]. The versatility of DEAs extends to fiber-shaped configurations, drawing inspiration from biological muscle structures and contributing to the development

Electroactive Polymer Actuators and Devices (EAPAD) XXVI, edited by
John D. W. Madden, Proc. of SPIE Vol. 12945, 129450O
 · 0277-786X · doi: 10.1117/12.3010130

of active textiles, exoskeletons, and precise gripping mechanisms. This innovation offers multifaceted utility in soft robotic systems, enhancing the scope of applications[11]–[18].

The role of the rcomposition (silicone polymer, crosslinker, catalyst, and reinforcing fillers)and the length of the polymer chain onthe stress-strain characteristics of silicone elastomers highlights the complex interplay of material composition and polymer dynamics. Adjustments in the ratio of these components and polymer chain lengths, along with the addition of multiple additives and fillers, are necessary for tailoring the mechanical integrity and elasticity of silicone elastomers. This enables their adaptation to a wide range of applications [19], [20]. The functionalization of silicone materials, through the incorporation of novel cross-linkers and chemical modifications, such as co-hydrosilylation, significantly boosts their thermal and dielectric performance, making them suitable for advanced electronic and biomaterial applications. The importance of post-curing processes for improved electro-mechanical stability is also highlighted, especially for commercial RTV and LSR elastomers, as it substantially enhances their properties, underscoring the necessity of post-curing for mechanical and electrical stability in dielectric applications [21]–[24] .

Moreover, the development of compliant electrodes for dielectric elastomer actuators (DEAs) is critical, with research exploring various technologies, including carbon-based electrodes, thin metallic films, and nanoparticle implantation. These efforts aim to find a balance between compliance, conductivity, manufacturability, and sensing capabilities, crucial for advancing DEA technology towards miniaturization, low-voltage operation, and broader commercial applications [25]. This summary encapsulates the interconnected research themes within material science focused on optimizing silicone elastomers and electrode designs for dielectric elastomer actuators, highlighting the continuous push towards innovative solutions in soft robotics and beyond.

This study focuses on the modeling of hollow fiber dielectric elastomer actuators (HFDEAs). It specifically concentrates on numerical modeling and experimental analysis of fibers, paralleling the methodologies and fabrications seen in references [26], but with a focus on fibers that fall within the microscale diameter and thickness range of 100 to 500 microns. This focus on microscale dimensions sets it apart from previous research on dielectric elastomer actuators documented in references [27]–[29]. This focus on sub-millimeter scale fibers represents a significant shift towards exploring the potentials and challenges associated with miniaturized dielectric elastomer actuators. Our system comprises a silicone tube filled with an ionic liquid electrode and carbon black serving as the external electrode. Preliminary mechanical and dielectric permittivity testing on the fabricated fibers ascertain their material properties, setting the stage for a comprehensive numerical model developed using COMSOL Multiphysics. This study not only investigates the actuation characteristics to validate the numerical model but also delves into the underlying reasons for strain behaviors and actuation forces through meticulous parameter validation, thus contributing to the broader understanding and optimization of HFDEAs.

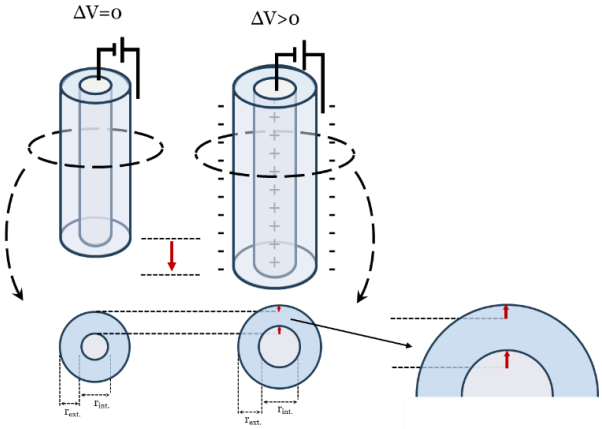

Figure 1. Working principles of HFDEA: changes in length, cross-section, and thickness before and after voltage application

2. METHODOLOGY

2.1 Materials

This study utilized a range of materials, including a [4-6% mercaptopropyl]methylsiloxane-dimethylsiloxane copolymer (SMS-042, molecular weight = 6869 g/mol, containing an average of 4.5 mercaptopropyl groups per molecule) and vinyl-terminated polydimethylsiloxane (DMS-V31, molecular weight = 28000 g/mol), both acquired from Gelest Inc., USA. Other chemicals, such as chloroform, 2,2-dimethoxy-2-phenylacetophenone (DMPA), 1-ethyl-3-methylimidazolium bis(trifluoromethylsulfonyl)imide ([Emim][TFSI]), ethanol, and acetone were sourced from VWR Chemicals BDH. Polyvinyl acetate (PVAc, molecular weight = 90000 g/mol) was sourced from Polysciences Inc., USA. The chemicals were used as received, without any additional purification processes.

2.2 Fabrication

2.2.1 Preparation of Silicone Fibers

Silicone elastomer fibers were produced through a thiol-ene click chemistry process, involving a reaction between vinyl-terminated polydimethylsiloxane (DMS-V31) and mercaptopropyl polydimethylsiloxane (SMS-042), with DMPA serving as the photoinitiator. This method was employed to ensure the effective polymerization of the silicone components. The production of silicone fibers was achieved through a wet spinning process, using a dual-needle coaxial spinneret. The apparatus for spinning was set up by submerging the spinneret 3 mm deep in an ethanol solution contained in a glass tube. The process involved simultaneously injecting ethanol and silicone solutions through the inner and outer needles, respectively. This was immediately followed by curing under UV light. The procedure controlled various parameters such as the distance from the UV source, the duration of exposure to UV light within the ethanol solution, and the spinning speed. Adjustments to the volume flow rate ratio of the inner solvent to the outer silicone solution allowed for the fabrication of silicone hollow fibers with varied wall thicknesses, the geometrical parameters of fibers are mentioned in Table 1.

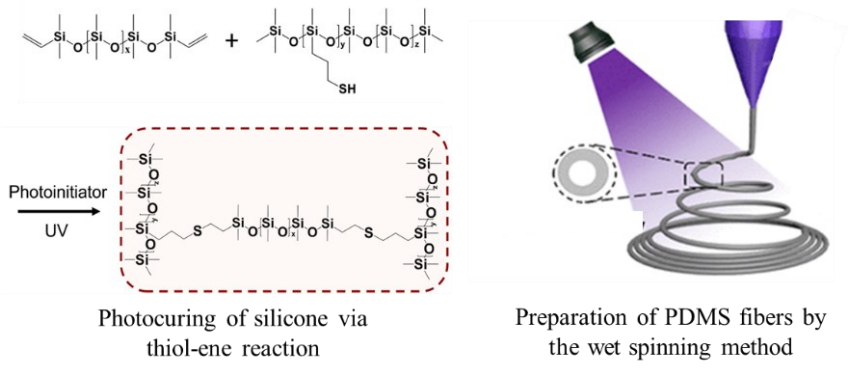

Figure 2. (left) The reaction involved in the crosslinking process and (right) the fabrication process of hollow fiber dielectric elastomer.[18]

2.2.2 Fabrication of Silicone Fiber Actuators

The assembly of silicone fiber actuators commenced with the injection of [Emim][TFSI] ionic liquid into the hollow silicone fibers, serving as the internal core electrode. Subsequently, a fine copper wire, designed to connect the ionic liquid core with the external high-voltage supply, was inserted into the fiber. The ends of the fiber were sealed using the same

silicone composition used in the fiber's fabrication, followed by exposure to UV light for sealing. The final step involved coating the exterior of the silicone fiber with carbon grease, establishing it as the outer conductive electrode.

Table 1. The prepared silicone fibers and their characteristics

Samples	Outer radius	Inner radius	Wall thickness
	(μm)	(μm)	(μm)
Fiber I	235	142	93
Fiber II	303	222	81

2.3 Characterization

2.3.1 Optical Analysis:

The structural features and thickness of the PDMS fibers were examined using an optical microscope (Leica DMLS, Germany).

2.3.2 Dielectric Permittivity:

Dielectric Relaxation Spectroscopy (DRS) analysis was conducted using a high-performance Novocontrol Alpha-A frequency analyzer (Novocontrol Technologies GmbH & Co, Germany), applying an electrical field of approximately 1 V/mm^{-1} across a frequency spectrum of 0.1 to 10^{-6} Hz, at ambient temperature. Copper sheets served as electrodes for the elastomers during the DRS analysis. The samples tested had a diameter of 20 mm and a thickness of 1 mm.

2.3.3 Mechanical Properties:

The Instron 3340 system (Instron, US) was used to measure tensile strength, strain at break, and Young's modulus. Samples were stretched at a rate of 10 mm per minute from an initial separation of 10 mm, with Young's modulus calculated from the stress-strain curve's slope at 20% strain. Results were averaged over three samples.

2.3.4 Actuation Performance:

Actuation was conducted with a Petapico-Voltron high-voltage power supply. Each fiber actuator was pre-strained by 20% using a 0.6 g weight and subjected to increasing voltage increments of 250 V up to 2 kV. Changes in fiber length were captured with a LUMIX DMC-G80 digital camera and analyzed using Tracker software for video analysis.

3. NUMERICAL MODEL

3.1 Theoretical Foundations of DEA Modeling

This section delves into the intricate energy concepts that govern the operation of DEAs. It begins by outlining the total energy equation of the DEA system, which incorporates mechanical strain energy from elastomer deformation, electrostatic energy from the applied electric field, and pre-stretched potential energy [28], [30]:

The total energy E_{total} of the DEA system is the sum of the mechanical strain energy (E_{mech}) derived from the deformation of the elastomer, the electrostatic energy (E_{elec}) due to the applied electric field and pre-stretched potential energy:

$$E_{\mathrm{total}} = E_{\mathrm{mech}} + E_{\mathrm{elec}} + E_{\mathrm{load}} \qquad (1)$$

For soft elastomers, multiple constitutive models exist[31], [32], for the mechanical part, using the two-parameter Mooney-Rivlin model, the strain energy density function W is given by:

$$W = C_{10}(I_1 - 3) + C_{01}(I_2 - 3) \quad (2)$$

where:

C_{10} and C_{01} are the material constants or parameters of the model. I_1 and I_2 are the first and second invariants of the Cauchy-Green deformation tensor, respectively. The invariants I_1 and I_2 are defined as:

$$I_1 = {\lambda_1}^2 + {\lambda_2}^2 + {\lambda_3}^2 \quad (3)$$

$$I_1 = ({\lambda_1}^2{\lambda_2}^2) + ({\lambda_2}^2{\lambda_3}^2) + ({\lambda_1}^2{\lambda_3}^2) \quad (4)$$

where λ_1 , λ_2 and λ_3 are the principal stretch ratios.

The mechanical energy (E_{mech}) is obtained by integrating the strain energy density W over the volume V of the elastomer:

$$E_{\text{mech}} = \int_V W dV \quad (5)$$

The electrostatic energy (E_{elec}) in the presence of an electric field E applied across the thickness d of the elastomer, assuming a homogeneous and isotropic dielectric material, can be expressed as:

$$E_{\text{elec}} = \frac{\varepsilon_0 \varepsilon_r}{2} \int_V E^2 dV \quad (6)$$

ε_0 is the vacuum permittivity constant ($8.854*10^{-12}$ F.m^{-1}), ε_r is the relative permittivity of the dielectric material, and E is the magnitude of the electric field, which can be related to the applied voltage V and the deformed thickness d of the DEA as $E=V/d$.

DEAs are often pre-stretched to guide their actuation response. To apply a pre-stretch in linear DEFAs, we loaded a weight to the fibers. This approach necessitates the inclusion of the load's potential energy, E_{load}, in the overall energy consideration:

$$E_{\text{load}} = -mgl_0(\lambda_l - 1) \quad (7)$$

In this context, m and g symbolize the mass of the load and the acceleration due to gravity, respectively. The negative sign indicates that the work was performed by the load.

3.2 Equilibrium State

The equilibrium state of the DEA is determined by minimizing the total energy (Eq. 1) with respect to the deformation, ensuring mechanical equilibrium under electrostatic actuation. This involves solving the equilibrium equations derived from the first derivative of the total energy (E_{total}) with respect to deformation, which encapsulates the coupling between mechanical and electrical domains within the geometric confines of the model in COMSOL Multiphysics which can be defined by the equation:

$$\frac{\partial E_{\text{total}}}{\partial \lambda_l} = 0 \quad (8)$$

Solving this equation for the equilibrium state involves identifying the local minimum of E_{total}, which yields the stretch ratio λ_l as a function of the applied voltage V. Consequently, the actuation strain s is determined by the relationship:

$$s(V) = \lambda_l(V) - 1 \qquad (9)$$

This formulation provides a comprehensive framework for simulating the complex behaviors of DEAs, allowing for the exploration of various design parameters and operating conditions to optimize the performance of these actuators.

3.3 Numerical Modeling Approach

For situations involving complex scenarios, such as large deformations, intricate material properties, or specific boundary conditions, numerical modeling becomes indispensable. In our study, we employed COMSOL Multiphysics for this purpose. COMSOL's powerful simulation environment allowed us to define the geometry and physics of the DEA, incorporating: Solid Mechanics**,** to simulate the mechanical behavior and deformations of the elastomer material. Electrostatics**,** to model the electric field distribution within the DEA and Electromechanical Forces, as a multiphysics coupling that captures the interaction between the DEA's mechanical and electrical properties. The simulation process began with the creation of a detailed mesh to discretize the DEA geometry, ensuring accurate representation of the physical domain. This step was critical for resolving the spatial variations in mechanical and electrical properties throughout the actuator. The initial state of the model was defined by specifying the material properties. For the mechanical aspect, a parameter investigation was conducted to select the most suitable hyperelastic material model. After evaluating both the Neo-Hookean and Mooney-Rivlin models, the latter was chosen based on its better fit (evidenced by a higher R-squared value) to the elastomer's nonlinear behavior. The remaining material properties were directly obtained from experimental measurements, ensuring a realistic simulation setup.

3.4 Parameter Investigation:

In order to accurately simulate the mechanical deformation of DE fibers, it is essential to employ a material model that captures the elastomer's nonlinear stress-strain behavior. First, we evaluate two hyperelastic material models. The first model is the Neo-Hookean model. The alternative model considered is the Mooney-Rivlin model, renowned for its simplicity and effectiveness, characterized by a two-parameter formulation.

Given that the Mooney-Rivlin model demonstrated a better fit to the purely mechanical properties, it was selected as the constitutive model. The stress-strain diagram and the fitting of the Mooney-Rivlin model are depicted in Fig. 3, while the fitted parameters of the model are presented in Table 2.

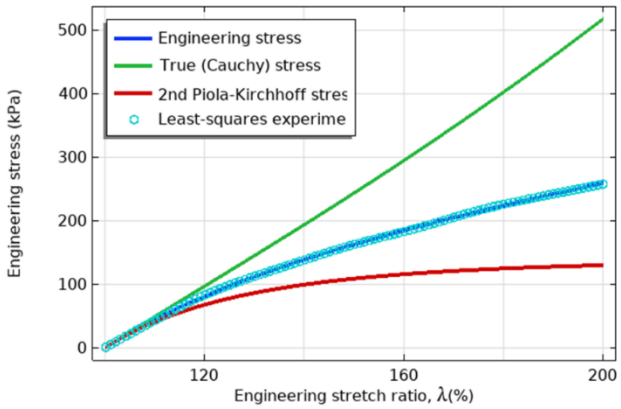

Figure 3. Mechanical characterization of hollow fiber dielectric elastomer: stress-stretch ratio analysis with Mooney-Rivlin fitting. The true (Cauchy) stress and second Piola-Kirchhoff stress are compared.

Table 2. Values of fitted parameters for the Mooney-Rivlin model, Eq. (2) .

Model	Parameters	
2-parameter Mooney-Rivlin	C_{01}=17.3 kPa	C_{10}=64.5 kPa

3.5 Experimental Validation:

To validate the computational model developed for HFDEAs, a direct comparison was conducted between the experimentally obtained actuation strains and those predicted by the model across a range of applied electric fields. This validation process is essential for verifying the model's accuracy in simulating the electro-mechanical response of DEAs, which is critical for their design and application in various fields.

4. RESULTS

In our investigation, we examined the behavior of hollow fiber Dielectric Elastomer actuators (HFDEA) under varying voltage conditions and pre-stretch applications. The study revealed a voltage-controllable elongation characteristic of the DE fibers, with actuation strain exhibiting a proportional increase alongside rising voltage levels, as depicted in Figure 5. This observed trend persisted across all pre-stretch conditions examined, indicating a consistent mechanical response to electrical stimulation.

The experimental outcomes demonstrated a quadratic relationship between actuation strain and applied voltage, as predicted by the Maxwell stress equation, $p = \frac{\varepsilon_0 \varepsilon_r}{2}(\frac{V}{d})^2$. This equation highlights a fundamental operational principle in DEAs, linking electrostatic forces to actuator deformation. Within the tested voltage spectrum, reaching up to 2 kV, the maximum actuation strains recorded were 4.1% and 2.5% for fibers I and II, respectively, under a pre-stretch condition of approximately 20% induced by a loading mechanism. In figure 4, a comparative analysis with numerical simulations revealed a matching trend between experimental observations and simulated outcomes, affirming the model's ability to replicate the stiffening effect under varying pre-stretch conditions. However, a discrepancy emerged in actuation strains, with simulated values consistently higher than those measured experimentally. This variance could potentially be attributed to the omission of various parameters, including the mechanical resistance of electrodes, dielectric losses, mechanical losses, and losses within the electrodes themselves..

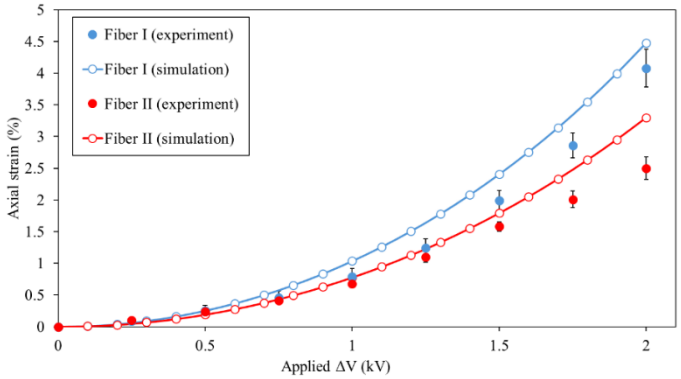

Figure 4. Axial strain as a function of electrical voltage: a comparison between experimental and simulation results

Figure 5 provides the radial strain as a function of applied voltage for both internal and external layers.An unexpected expansion of the external radius was recorded. This phenomenon – which is visualized in figure 6- is rationalized by the differential surface charge density between the internal and external layers, as highlighted in Figure 7, where the internal layer exhibits a higher charge density upon voltage application, leading to the experimentally observed radial expansion.

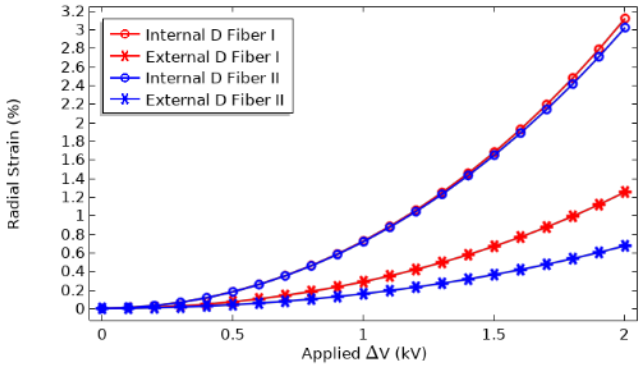

Figure 5. Simulation results: radial strain response to varying electric voltage. The internal and external radial strains under different voltage levels are compared.

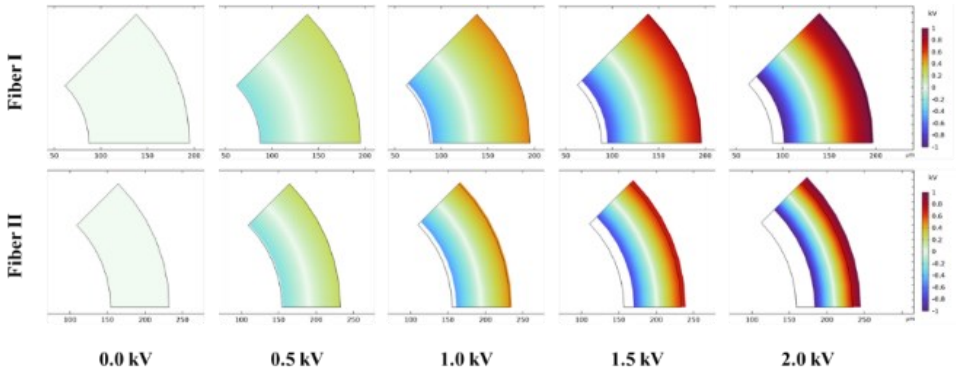

Figure 6. Simulation results: This figure displays the electric potential gradient along the cross-section of fibers. Additionally, to enhance clarity, the deformation is visually exaggerated by a factor of 5.

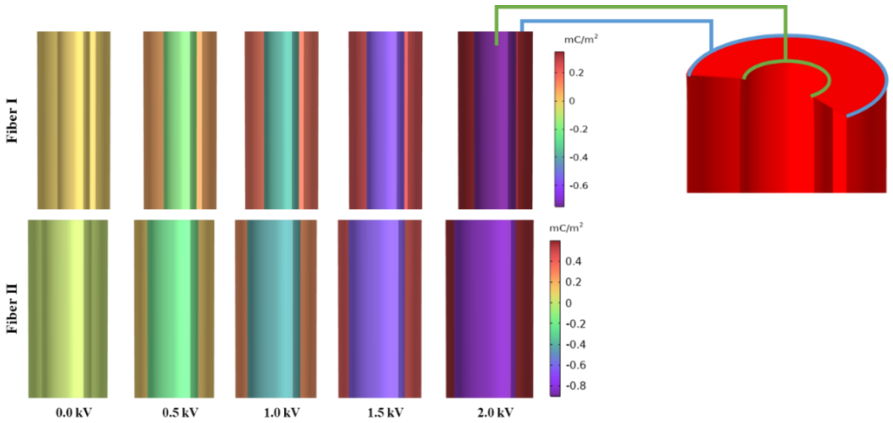

Figure 7. Simulation results: Comparison of surface charge density on internal vs. external layers of HFDEAs. This figure illustrates a higher surface charge density along the internal boundary compared to the external boundary.

In the next step of our investigation, we investigated how design parameters affect the actuation strain of HFDEAs, focusing on the effects of changing the internal diameter while keeping the wall thickness the same. This study aimed to make clear the relationship between changes in the internal geometry and the actuator's performance.

Our findings, illustrated in Figure 8, demonstrate that enlarging the internal diameter of HFDEAs initially enhances axial strain, attributed to the expanded internal cavity facilitating greater electrostatically driven expansion. Nonetheless, there exists an optimal diameter range beyond which further enlargement does not appreciably augment axial strain, indicating a balance between electrostatic forces and the material's structural integrity. Similarly, while the external radial strain increases with larger diameters, benefiting from reduced internal pressure constraints, it too reaches a plateau, suggesting a limit to the benefits of diameter enlargement. In contrast, as the internal diameter increases, the internal radial strain decreases and eventually plateaus. This pattern highlights how the effectiveness of surface charge density diminishes with larger diameters, leading to a less responsive strain.

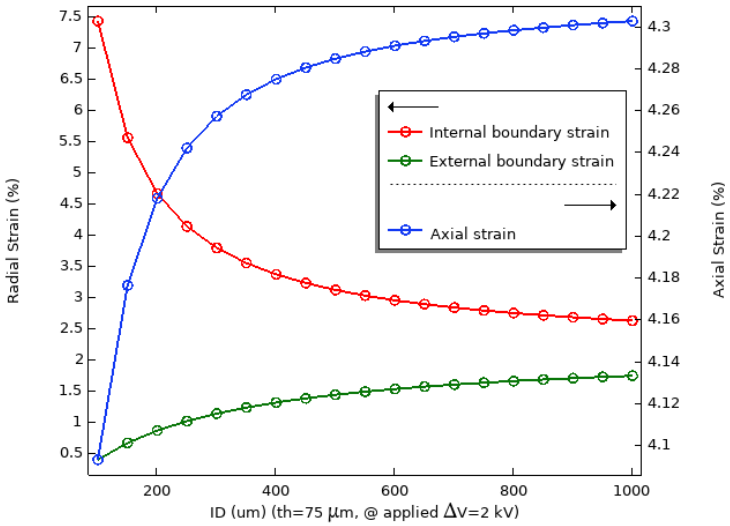

Figure 8. Simulation results on the effect of internal diameter on actuation strain in HFDEAs at 2 kV applied voltage. This figure illustrates the relationship between varying internal diameters and the performance of the actuator across different strain measures, while the wall thickness remains constant.

5. CONCLUSIONS

This study has advanced our understanding of the design parameters affecting hollow fiber dielectric elastomer actuator (HFDEAs), leveraging both experimental insights and numerical simulations. We identified how actuation strain in HFDEAs responds to variations in applied voltage and pre-stretch conditions, highlighting the voltage-controlled elongation capabilities of these actuators. Our research confirmed the quadratic relationship between actuation strain and voltage, guided by the Maxwell stress equation.

While experimental results align closely with computational predictions, discrepancies in actuation strain underscore the necessity for model refinement, especially in incorporating electrode effects. Insights into the impact of internal diameter adjustments on actuation strain underscore the significance of geometrical considerations in DEA design, revealing a critical threshold for diameter enlargement beyond which performance gains level off.

In essence, our findings offer valuable guidelines for optimizing HFDEA design, emphasizing the importance of balancing geometrical configurations to enhance actuator performance. Future directions will aim at refining computational models and exploring new materials, with the goal of broadening DEA applications in soft robotics and beyond.

ACKNOWLEDGEMENTS

The Novo Nordisk Foundation is acknowledged for its generous funding through the Challenge Program, grant no NNF22OC0071130.

REFRENCES

[1] D. Rus and M. T. Tolley, "Design, fabrication and control of soft robots," *Nature*, vol. 521, no. 7553, pp. 467–475, May 2015, doi: 10.1038/NATURE14543.

[2] S. I. Rich, R. J. Wood, and C. Majidi, "Untethered soft robotics," *Nat. Electron. 2018 12*, vol. 1, no. 2, pp. 102–112, Feb. 2018, doi: 10.1038/s41928-018-0024-1.

[3] J. Shintake, V. Cacucciolo, D. Floreano, and H. Shea, "Soft Robotic Grippers," *Adv. Mater.*, vol. 30, no. 29, p. 1707035, Jul. 2018, doi: 10.1002/ADMA.201707035.

[4] Y. Guo, L. Liu, Y. Liu, and J. Leng, "Review of Dielectric Elastomer Actuators and Their Applications in Soft Robots," *Adv. Intell. Syst.*, vol. 3, no. 10, 2021, doi: 10.1002/aisy.202000282.

[5] U. Gupta *et al.*, "Soft robots based on dielectric elastomer actuators: a review," *SMaS*, vol. 28, no. 10, p. 103002, Sep. 2019, doi: 10.1088/1361-665X/AB3A77.

[6] G. Y. Gu, J. Zhu, L. M. Zhu, and X. Zhu, "A survey on dielectric elastomer actuators for soft robots," *Bioinspir. Biomim.*, vol. 12, no. 1, Feb. 2017, doi: 10.1088/1748-3190/12/1/011003.

[7] E. Hajiesmaili and D. R. Clarke, "Dielectric elastomer actuators," *J. Appl. Phys.*, vol. 129, no. 15, p. 151102, Apr. 2021, doi: 10.1063/5.0043959/1025587.

[8] X. Ji *et al.*, "An autonomous untethered fast soft robotic insect driven by low-voltage dielectric elastomer actuators," *Sci. Robot.*, vol. 4, no. 37, Dec. 2019, doi: 10.1126/SCIROBOTICS.AAZ6451.

[9] P. Brochu and Q. Pei, "Advances in dielectric elastomers for actuators and artificial muscles," *Macromol. Rapid Commun.*, vol. 31, no. 1, pp. 10–36, Jan. 2010, doi: 10.1002/MARC.200900425.

[10] T. Li, C. Keplinger, R. Baumgartner, S. Bauer, W. Yang, and Z. Suo, "Giant voltage-induced deformation in dielectric elastomers near the verge of snap-through instability," *J. Mech. Phys. Solids*, vol. 61, no. 2, pp. 611–628, Feb. 2013, doi: 10.1016/J.JMPS.2012.09.006.

[11] R. W. Jones *et al.*, "An arm wrestling robot driven by dielectric elastomer actuators," *Smart Mater. Struct.*, vol. 16, no. 2, p. S306, Mar. 2007, doi: 10.1088/0964-1726/16/2/S16.

[12] G. Kovacs, L. Düring, S. Michel, and G. Terrasi, "Stacked dielectric elastomer actuator for tensile force transmission," *Sensors Actuators A Phys.*, vol. 155, no. 2, pp. 299–307, Oct. 2009, doi: 10.1016/J.SNA.2009.08.027.

[13] O. A. Araromi *et al.*, "Rollable multisegment dielectric elastomer minimum energy structures for a deployable microsatellite gripper," *IEEE/ASME Trans. Mechatronics*, vol. 20, no. 1, pp. 438–446, 2015, doi: 10.1109/TMECH.2014.2329367.

[14] S. Kurumaya, K. Suzumori, H. Nabae, and S. Wakimoto, "Musculoskeletal lower-limb robot driven by multifilament muscles," *ROBOMECH J.*, vol. 3, no. 1, pp. 1–15, Dec. 2016, doi: 10.1186/s40648-016-0061-3.

[15] S. Kurumaya, H. Nabae, G. Endo, and K. Suzumori, “Active Textile Braided in Three Strands with Thin McKibben Muscle,” *Soft Robot.*, vol. 6, no. 2, pp. 250–262, Apr. 2019, doi: 10.1089/soro.2018.0076.

[16] N. Thompson, X. Zhang, F. Ayala, E. T. Hsiao-Wecksler, and G. Krishnan, “Augmented Joint Stiffness and Actuation Using Architectures of Soft Pneumatic Actuators,” *Proc. - IEEE Int. Conf. Robot. Autom.*, pp. 1533–1538, Sep. 2018, doi: 10.1109/ICRA.2018.8460746.

[17] N. R. Sinatra, C. B. Teeple, D. M. Vogt, K. K. Parker, D. F. Gruber, and R. J. Wood, “Ultragentle manipulation of delicate structures using a soft robotic gripper,” *Sci. Robot.*, vol. 4, no. 33, p. 5425, Aug. 2019, doi: 10.1126/scirobotics.aax542.

[18] Z. Kang, L. Yu, Y. Nie, M. Skowyra, S. Zhang, and A. L. Skov, “Fiber-Format Dielectric Elastomer Actuators by the Meter,” *Adv. Funct. Mater.*, p. 2314056, Feb. 2024, doi: 10.1002/ADFM.202314056.

[19] P. Mazurek, S. Vudayagiri, and A. L. Skov, “How to tailor flexible silicone elastomers with mechanical integrity: A tutorial review,” *Chemical Society Reviews*, vol. 48, no. 6. Royal Society of Chemistry, pp. 1448–1464, Mar. 21, 2019. doi: 10.1039/c8cs00963e.

[20] M. F. Koziol, P. L. Nguyen, S. Gallo, B. D. Olsen, and S. Seiffert, “Hierarchy of relaxation times in supramolecular polymer model networks,” *Phys. Chem. Chem. Phys.*, vol. 24, no. 8, pp. 4859–4870, Feb. 2022, doi: 10.1039/D1CP04213K.

[21] F. B. Madsen, I. Dimitrov, A. E. Daugaard, S. Hvilsted, and A. L. Skov, “Novel cross-linkers for PDMS networks for controlled and well distributed grafting of functionalities by click chemistry,” *Polym. Chem.*, vol. 4, no. 5, pp. 1700–1707, Feb. 2013, doi: 10.1039/C2PY20966G.

[22] C. Racles, M. Alexandru, A. Bele, V. E. Musteata, M. Cazacu, and D. M. Opris, “Chemical modification of polysiloxanes with polar pendant groups by co-hydrosilylation,” *RSC Adv.*, vol. 4, no. 71, pp. 37620–37628, Aug. 2014, doi: 10.1039/C4RA06955B.

[23] F. B. Madsen, A. E. Daugaard, S. Hvilsted, and A. L. Skov, “The Current State of Silicone-Based Dielectric Elastomer Transducers,” *Macromol. Rapid Commun.*, vol. 37, no. 5, pp. 378–413, Mar. 2016, doi: 10.1002/MARC.201500576.

[24] S. Zakaria, F. B. Madsen, and A. L. Skov, “Post Curing as an Effective Means of Ensuring the Long-term Reliability of PDMS Thin Films for Dielectric Elastomer Applications,” *Polym. Plast. Technol. Eng.*, vol. 56, no. 1, pp. 83–95, Jan. 2017, doi: 10.1080/03602559.2016.1211689.

[25] S. Rosset and H. R. Shea, “Flexible and stretchable electrodes for dielectric elastomer actuators,” *Appl. Phys. A Mater. Sci. Process.*, vol. 110, no. 2, pp. 281–307, Feb. 2013, doi: 10.1007/s00339-012-7402-8.

[26] Z. Kang, L. Yu, and A. L. Skov, “Transparent PDMS fiber actuator with ionic liquid-based electrodes,” SPIE-Intl Soc Optical Eng, Apr. 2023, p. 9. doi: 10.1117/12.2655769.

[27] F. Carpi and D. De Rossi, “Dielectric elastomer cylindrical actuators: Electromechanical modelling and experimental evaluation,” *Mater. Sci. Eng. C*, vol. 24, no. 4, pp. 555–562, Jun. 2004, doi: 10.1016/j.msec.2004.02.005.

[28] T. Lu, C. Ma, and T. Wang, “Mechanics of dielectric elastomer structures: A review,” *Extrem. Mech. Lett.*, vol. 38, p. 100752, 2020, doi: 10.1016/j.eml.2020.100752.

[29] S. Arora, T. Ghosh, and J. Muth, “Dielectric elastomer based prototype fiber actuators,” *Sensors Actuators A Phys.*, vol. 136, no. 1, pp. 321–328, May 2007, doi: 10.1016/J.SNA.2006.10.044.

[30] Z. Suo, “THEORY OF DIELECTRIC ELASTOMERS,” *China Acta Mech. Solida Sin.*, vol. 23, no. 6, 2010, doi: 10.1016/S0894-9166(11)60004-9.

[31] P. Hu, J. Madsen, Q. Huang, and A. L. Skov, “Elastomers without covalent cross-linking: Concatenated rings giving rise to elasticity,” *ACS Macro Lett.*, vol. 9, no. 10, pp. 1458–1463, Oct. 2020, doi: 10.1021/acsmacrolett.0c00635.

[32] P. Hu, J. Madsen, and A. L. Skov, “One reaction to make highly stretchable or extremely soft silicone elastomers from easily available materials,” *Nat. Commun. 2022 131*, vol. 13, no. 1, pp. 1–10, Jan. 2022, doi: 10.1038/s41467-022-28015-2.